University of Massachusetts Amherst

From the SelectedWorks of David M Ford

April, 2005

Inverse density functional theory as an interpretive tool for measuring colloid-surface interactions in dense systems

David M Ford, *University of Massachusetts - Amherst*
Mingqing Lu
Michael A Bevan

Available at: https://works.bepress.com/david_ford/1/

bepress™

Inverse density-functional theory as an interpretive tool for measuring colloid-surface interactions in dense systems

Mingqing Lu, Michael A. Bevan, and David M. Ford

Citation: J. Chem. Phys. **122**, 224710 (2005); doi: 10.1063/1.1929734
View online: http://dx.doi.org/10.1063/1.1929734
View Table of Contents: http://jcp.aip.org/resource/1/JCPSA6/v122/i22
Published by the American Institute of Physics.

Additional information on J. Chem. Phys.

Journal Homepage: http://jcp.aip.org/
Journal Information: http://jcp.aip.org/about/about_the_journal
Top downloads: http://jcp.aip.org/features/most_downloaded
Information for Authors: http://jcp.aip.org/authors

ADVERTISEMENT

Downloaded 09 Jul 2012 to 128.119.169.61. Redistribution subject to AIP license or copyright; see http://jcp.aip.org/about/rights_and_permissions

HTML ABSTRACT + LINKS

Inverse density-functional theory as an interpretive tool for measuring colloid-surface interactions in dense systems

Mingqing Lu, Michael A. Bevan, and David M. Ford[a)]
Department of Chemical Engineering, Texas A&M University, College Station, Texas 77843-3122

(Received 28 March 2005; accepted 18 April 2005; published online 15 June 2005)

Recent advances in optical microscopy, such as total internal reflection and confocal scanning laser techniques, now permit the direct three-dimensional tracking of large numbers of colloidal particles both near and far from interfaces. A novel application of this technology, currently being developed by one of the authors under the name of diffusing colloidal probe microscopy (DCPM), is to use colloidal particles as probes of the energetic characteristics of a surface. A major theoretical challenge in implementing DCPM is to obtain the potential energy of a single particle in the external field created by the surface, from the measured particle trajectories in a dense colloidal system. In this paper we develop an approach based on an inversion of density-functional theory (DFT), where we calculate the single-particle-surface potential from the experimentally measured equilibrium density profile in a nondilute colloidal fluid. The underlying DFT formulation is based on the recent work of Zhou and Ruckenstein [Zhou and Ruckenstein, J. Chem. Phys. **112**, 8079 (2000)]. For model hard-sphere and Lennard-Jones systems, using Monte Carlo simulation to provide the "experimental" density profiles, we found that the inversion procedure reproduces the true particle-surface-potential energy to an accuracy within typical DCPM experimental limitations ($\sim 0.1kT$) at low to moderate colloidal densities. The choice of DFT closures also significantly affects the accuracy. © *2005 American Institute of Physics*. [DOI: 10.1063/1.1929734]

I. INTRODUCTION

A. Diffusing colloidal probe microscopy

Diffusing colloidal probe microscopy (DCPM) is an emerging surface analysis technique currently being developed by one of the authors.[1] In DCPM, an ensemble of freely diffusing colloidal particles are employed as ultrasensitive probes of a nearby surface. Total internal reflection[2]- and video[3]-based optical microscopy techniques, which combine the scattering of an evanescent wave with standard image capture and analysis algorithms, are used to monitor the three-dimensional Brownian excursions of the colloidal particles as they sample spatial positions over time. Confocal scanning laser microscopy[4] methods are also being developed to measure three-dimensional colloidal trajectories near surfaces. The particle trajectories may then be analyzed as time-averaged distribution functions using statistical mechanical interpretations to yield the relative potential energy of a single colloidal particle as a function of *xyz* position near the surface (the main goal of this paper). If the surface is known to be a chemically and physically uniform plane, only the surface normal direction z is important and the analysis is consequently simplified.

Because DCPM exploits colloidal Brownian motion as a natural gauge of potential-energy landscapes, it is inherently capable of measuring energies and forces 10^3 times weaker than the range accessible using "top down" methods employing external mechanical manipulation (i.e., scanning probes, optical tweezers).[2] Preliminary work[1] has successfully implemented DCPM to perform ensemble measurements in model synthetic systems, and the technique is currently being extended to measure specific equilibrium interactions between protein pairs covalently attached to metal nanoparticles and planar substrate surfaces.

B. Theoretical requirements

The main goal of this paper is to develop a theoretical approach that yields an accurate single-particle-surface potential based on information extracted from particle distribution functions measured using DCPM. Density-functional theory (DFT) is a logical choice for this purpose. One of the key expectations underlying DFT is a unique correspondence between a density profile and the underlying particle and surface pair potentials.[5] Thus, we expect that if we extract an equilibrium density profile $\rho(\mathbf{r})$ from the DCPM measured particle trajectories, we can invert it to obtain the colloid-surface potential $\varphi_{\text{ext}}(\mathbf{r})$ using the fundamentals of DFT. Subject to spatial and temporal sampling limitations, the DCPM technique indeed produces histograms[1] that may be normalized to produce density profiles. This paper focuses on the development of an inverse DFT approach that is (1) accurate to within the inherent experimental limitations of DCPM, typically on the order of $0.1kT$, (2) fast enough to report a surface potential within minutes on a computer workstation, and (3) systematically adaptable to a range of different particle and surface types.

[a)]Author to whom correspondence should be addressed. Fax: (979) 845-6446; electronic mail: d-ford@chemail.tamu.edu

 © 2005 American Institute of Physics

Downloaded 09 Jul 2012 to 128.119.169.61. Redistribution subject to AIP license or copyright; see http://jcp.aip.org/about/rights_and_permissions

C. Present work

The paper is organized as follows. Section II outlines the theoretical approach, including a brief review of the recent DFT formulation of Zhou and Ruckenstein.[6] Section III describes the model systems on which the inverse approach is tested and the Monte Carlo techniques used to generate simulated DCPM data. (Actual experimental data were not used in this paper but will be in future publications). Section IV contains the results and discussion, and Sec. V summarizes the conclusions.

II. THEORY

A. Forward analysis

In this subsection we provide a brief review of the traditional forward problem of DFT, i.e., the calculation of fluid structure based on a specified external field. Emphasis is given to the perturbative DFT formulation recently presented by Zhou and Ruckenstein.[6] The density profile of a single-component fluid in an inhomogeneous environment is generally written as

$$\rho(\mathbf{r}) = \rho_b \exp[-\beta\varphi_{\mathrm{ext}}(\mathbf{r}) + C^{(1)}(\mathbf{r};[\rho]) - C_0^{(1)}(\rho_b)], \tag{1}$$

where $\rho(\mathbf{r})$ is the density profile, ρ_b is the bulk density, $\varphi_{\mathrm{ext}}(\mathbf{r})$ is the potential energy of the external field, $\beta = 1/kT$ with k the Boltzmann constant and T the absolute temperature, $C^{(1)}(\mathbf{r};[\rho])$ is the first-order direct correlation function of the nonuniform fluid, and $C_0^{(1)}(\rho_b)$ is the corresponding quantity in the bulk fluid. The essence of the forward DFT problem is to develop an estimate for $C^{(1)}(\mathbf{r};[\rho])$ based on the imposed $\varphi_{\mathrm{ext}}(\mathbf{r})$ and ρ_b, so that $\rho(\mathbf{r})$ may be obtained via Eq. (1). We note that the external potential could arise from various sources, such as the presence of a surface or the application of a gravitational or electromagnetic field (or some combination thereof).

In the methodology of perturbative DFT, $C^{(1)}(\mathbf{r};[\rho])$ is expanded around the uniform system of bulk density as

$$\begin{aligned} C^{(1)}(\mathbf{r};[\rho]) = C_0^{(1)}(\rho_b) &+ \int d\mathbf{r}_1[\rho(\mathbf{r}_1) - \rho_b] C_0^{(2)}(\mathbf{r},\mathbf{r}_1;\rho_b) \\ &+ \sum_{n=3}^{\infty} \frac{1}{(n-1)!} \int d\mathbf{r}_1 \int d\mathbf{r}_2 \cdots \int d\mathbf{r}_{n-1} \\ &\times \prod_{m=1}^{n-1} [\rho(\mathbf{r}_m) - \rho_b] C_0^{(n)}(\mathbf{r},\mathbf{r}_1,\cdots\mathbf{r}_{n-1};\rho_b), \end{aligned} \tag{2}$$

where $C_0^{(n)}(\mathbf{r},\mathbf{r}_1,\cdots,\mathbf{r}_{n-1};\rho_b)$ is the n-order direct correlation function of a uniform fluid at bulk density ρ_b. Perturbative approaches usually focus on truncating this expansion at some reasonable order and evaluating the remaining direct correlation functions.[7] Recently Zhou and Ruckenstein[6] invoked the universality of the Helmholtz free-energy functional for systems with pairwise-additive interactions to show that Eq. (2) may be written much more concisely as

$$\begin{aligned} C^{(1)}(\mathbf{r};[\rho]) = C_0^{(1)}(\rho_b) &+ \int d\mathbf{r}_1[\rho(\mathbf{r}_1) - \rho_b] C_0^{(2)}(\mathbf{r},\mathbf{r}_1;\rho_b) \\ &+ B[\vartheta(\mathbf{r})], \end{aligned} \tag{3}$$

where the $n \geqslant 3$ terms are identified as the bridge function B of the fluid. (We note that the bridge function is the sum of the "elementary diagrams" in the integral equation theory literature.[8]) Here B is written as a functional of a yet-to-be-chosen structural correlation function $\vartheta(\mathbf{r})$; the functional relationship represents a closure in the sense of Ornstein–Zernike (OZ) integral equation theory. Zhou and Ruckenstein[6] point out that a natural choice of $\vartheta(\mathbf{r})$ for confined fluids is the inhomogeneous analogue of the bulk indirect correlation function, $\gamma(\mathbf{r}) = \int d\mathbf{r}_1(\rho(\mathbf{r}_1) - \rho_b) C_0^{(2)}(\mathbf{r},\mathbf{r}_1;\rho_b)$. With these choices, Eq. (1) becomes

$$\rho(\mathbf{r}) = \rho_b \left\{ \begin{aligned} &-\beta\varphi_{\mathrm{ext}}(\mathbf{r}) + \int d\mathbf{r}_1(\rho(\mathbf{r}_1) - \rho_b) C_0^{(2)}(\mathbf{r},\mathbf{r}_1;\rho_b) \\ &+ B\left[\int d\mathbf{r}_1(\rho(\mathbf{r}_1) - \rho_b) C_0^{(2)}(\mathbf{r},\mathbf{r}_1;\rho_b) \right] \end{aligned} \right\}. \tag{4}$$

Equation (4) is a novel formulation of DFT that predicts the density profile based purely on the bulk second-order direct correlation function and the choice of a closure relationship for the bridge function. Since the theory is perturbative, it requires no density weighting; unlike previous perturbative approaches, painstaking evaluation of higher-order correlation functions is not needed. The accuracy of the theory has been tested in several cases and found to be similar to that of the best previous DFT formulations. Zhou and Ruckenstein[6] initially examined single-component hard-sphere fluids confined to several different geometries and with different surface potentials. The theory has since been tested on different model fluids (e.g., Lennard-Jones,[9,10] Yukawa,[11] and penetrable spheres[12]), mixtures,[9,13] and polymers[14] with a high degree of success.

B. Inverse analysis

Our goal in this investigation is the inverse of the usual goal of DFT calculations. We assume that we can measure the density profile $\rho(\mathbf{r})$ of a dense fluid (e.g., a colloidal dispersion) in an inhomogeneous environment (e.g., near a surface), and we would like to use this information to predict the potential energy of a single colloidal particle at different locations in that environment, $\varphi_{\mathrm{ext}}(\mathbf{r})$. Algebraic inversion of Eq. (4) provides an equation for this purpose

$$\begin{aligned} \beta\varphi_{\mathrm{ext}}(\mathbf{r}) = &\int d\mathbf{r}_1(\rho(\mathbf{r}_1) - \rho_b) C_0^{(2)}(\mathbf{r},\mathbf{r}_1;\rho_b) \\ &+ B\left[\int d\mathbf{r}_1(\rho(\mathbf{r}_1) - \rho_b) C_0^{(2)}(\mathbf{r},\mathbf{r}_1;\rho_b) \right] \\ &- \ln[\rho(\mathbf{r})/\rho_b]. \end{aligned} \tag{5}$$

Every quantity on the right-hand side of Eq. (5) may be considered an input. We assume that the density profile and bulk density will be measured in the experiment. We also

Downloaded 09 Jul 2012 to 128.119.169.61. Redistribution subject to AIP license or copyright; see http://jcp.aip.org/about/rights_and_permissions

assume that the bulk second-order direct correlation function $C_0^{(2)}(\mathbf{r},\mathbf{r}_1;\rho_b)$ may be obtained "offline" from a separate consideration of the bulk fluid. For example, a video or confocal microscopy experiment could be done to directly measure the radial distribution function $g(\mathbf{r})$, and $C_0^{(2)}(\mathbf{r},\mathbf{r}_1;\rho_b)$ would then be accessible as the only unknown in the bulk OZ equation. Alternatively, the pairwise potential of mean force between particles could be obtained from a combination of total internal reflection microscopy and first-principles calculation,[15] and the bulk OZ equation could be solved in an appropriate closure to yield $C_0^{(2)}(\mathbf{r},\mathbf{r}_1;\rho_b)$. In either case, the unknown $\varphi_{\text{ext}}(\mathbf{r})$ may be obtained by the straightforward numerical operations shown in Eq. (5).

An analogous inverse problem arises for homogeneous fluids, and we note its parallel with the current problem. For homogeneous fluids of particles (either atomistic or colloidal), one would often like to deduce the pairwise particle–particle interaction potential from the experimentally determined radial distribution function $g(r)$.[16] If we consider the inhomogenous potential $\varphi_{\text{ext}}(\mathbf{r})$ to be caused by a single fluid particle located at the origin so that $\rho(\mathbf{r})=\rho_b g(\mathbf{r})$, then Eq. (5) reduces exactly to the diagrammatic modified hypernetted-chain (MHNC) formulation of the fluid structure inversion problem presented by Rosenfeld and Kahl.[16] In fact, Zhou and Ruckenstein[6] appeal to the concept of a single-particle inhomogeneity to derive Eq. (4). Since our mathematical formulation is analogous to that for structure-potential inversion problems in homogeneous fluids, we should be able to take advantage of techniques from that literature to improve the accuracy.[17]

The inversion of Zhou and Ruckenstein's theory embodied in Eq. (5) is well suited to our needs. The integral equation formulation carries a low computational burden. We expect that the necessary bulk fluid direct correlation functions will be easily obtainable from the same type of imaging techniques that produce the density profiles. Increased accuracy may be achieved through systematic improvements in closures or the application of techniques from the structure-potential inversion literature.

C. Simulated experiments

As a first test of the theory, we used Monte Carlo (MC) simulation to produce the density profiles to be used as the "experimental" input. Canonical MC (Ref. 18) was used to produce a set of appropriate equilibrium particle configurations for analysis. In this paper, we restricted ourselves to particles near a chemically and physically uniform planar surface (see Sec. III below). For convenience in the simulations, we used a slit-pore type of geometry with two identical surfaces placed at $z=0$ and $z=L$. The separation L was always large enough so that the density decayed to the bulk value in a plateau region around the center of the pore, so we essentially had two replicates of a single-surface study in each simulation. Periodic boundary conditions were used in the x and y directions. The number of particles was chosen to produce the correct bulk density in each case and ranged from 300 to 13 500. The number of production MC cycles was at least five million in each case. The density profiles were obtained with bins of width 0.05σ in the z direction (the definition of σ is given in Sec. III A below).

The only external fields in this study are the surface-particle potentials arising from the presence of the model surfaces; no other types of field, such as gravitational or electromagnetic, were included. Gravitational effects[19] will be considered in future papers where experimental data are employed. (We further note that the effects of a gravitational field can be practically removed from experiments by density matching the particles and medium, so the present model systems are not unrealistic.)

D. Procedure

Our general procedure for converting density profile information to a single-particle potential-energy function is outlined here. Specific models are described in the next section.

(1) Choose a model fluid and a potential-energy function $\varphi_{\text{ext}}(\mathbf{r})$ that represents the interaction of a single fluid particle with an external field. Choose a bulk density ρ_b and a temperature T for the fluid.
(2) Generate a density profile $\rho(\mathbf{r})$ by canonical Monte Carlo under the conditions chosen in step (1).
(3) Use the method of Labik *et al.*[20] to solve the OZ equation with an appropriate closure (e.g., Percus–Yevick, hypernetted chain) and obtain the direct correlation function $C_0^{(2)}(\mathbf{r};\rho_b)$ for the bulk model fluid.
(4) Use the bulk density from step (1), the density profile from step (2), and the bulk direct correlation function from step (3) to calculate the inhomogeneous indirect correlation function $\gamma(\mathbf{r})=\int d\mathbf{r}_1(\rho(\mathbf{r}_1)-\rho_b)\times C_0^{(2)}(\mathbf{r},\mathbf{r}_1;\rho_b)$.
(5) Choose an appropriate functional relationship (closure) for the bridge function $B[\gamma]$ and evaluate the right-hand side of Eq. (5) to yield a prediction of the potential energy $\varphi_{\text{ext}}^{\text{pred}}(\mathbf{r})$.
(6) Compare $\varphi_{\text{ext}}^{\text{pred}}(\mathbf{r})$ with the $\varphi_{\text{ext}}(\mathbf{r})$ imposed in step (1).

Note that we have two different places where a closure is used: in step (3) to obtain the direct correlation function for the homogenous fluid, and in step (5) to determine the bridge function for the inhomogeneous fluid. It is not necessary to choose the same closure for both steps. In the results, the choice for each step will be clearly noted.

III. MODEL SYSTEMS

A. Model fluids and surfaces

In this paper, the model fluid was always hard spheres of diameter σ. The external field was always created by a single planar surface, yielding inhomogeneity in the z direction only. Two different surface models were used. The first was a hard wall

$$\varphi_{\text{ext}}(z)=\begin{cases}\infty, & z<\sigma/2\\ 0, & z\geqslant\sigma/2\end{cases} \tag{6}$$

and the second was a Lennard-Jones 9-3 surface

Downloaded 09 Jul 2012 to 128.119.169.61. Redistribution subject to AIP license or copyright; see http://jcp.aip.org/about/rights_and_permissions

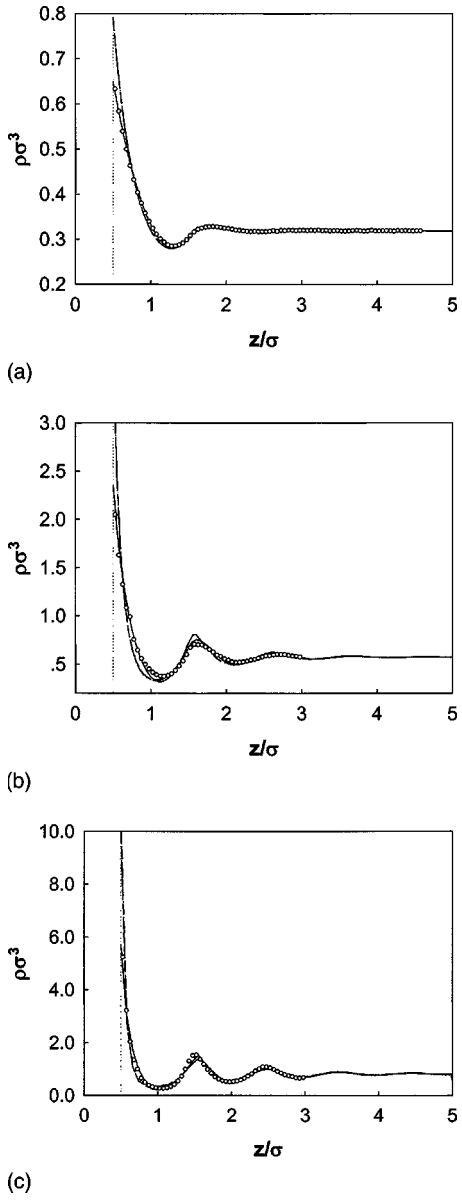

FIG. 1. Density profiles of hard-sphere fluids in contact with a hard planar surface, for bulk densities $\rho_b\sigma^3$ of (a) 0.319, (b) 0.5745, and (c) 0.813. In each case, the solid line was obtained using Eq. (4) with the PY closure for the bulk direct correlation function and VM for the bridge function (PY+VM). The dashed line and dash-dot-dot lines are for the VM+HNC and PY+HNC combinations, respectively. The open circles are the Monte Carlo simulation results. The vertical dotted line denotes the point of particle-surface contact.

$$\varphi_{\text{ext}}(z) = \varepsilon[(z_0/z)^9 - (z_0/z)^3], \tag{7}$$

where $z_0 = 0.71\sigma$ and $\varepsilon/k_B = 481$ K. In all simulations reported here, T was chosen to be 100 K. These models and conditions were chosen to match systems previously studied by MC simulation and DFT.[21]

B. Closures

The three closures employed in this work have analytical expressions for $B[\gamma]$, as summarized by Zhou and Ruckenstein.[6]

$$\text{Percus–Yevick (PY):} \quad B[\gamma(\mathbf{r})] = \ln(1+\gamma(\mathbf{r})) - \gamma(\mathbf{r}), \tag{8}$$

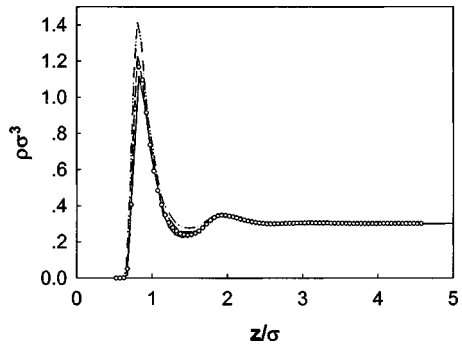

FIG. 2. Density profiles of hard-sphere fluids in contact with a Lennard-Jones 9-3 surface. The bulk density $\rho_b\sigma^3$ is 0.3; the potential model and parameter values are given in the text. As in Fig. 1, the solid, dashed, and dash-dot-dot lines denote the PY+VM, VM+HNC, and PY+HNC closure combinations, respectively. The open circles are the Monte Carlo simulation results.

$$\text{Verlet modified (VM):} \quad B[\gamma(\mathbf{r})] = -\gamma(\mathbf{r})^2/2(1+0.8\gamma(\mathbf{r})), \tag{9}$$

$$\text{Hypernetted chain (HNC):} \quad B[\gamma(\mathbf{r})] = 0. \tag{10}$$

IV. RESULTS AND DISCUSSION

For each model system, we initially solved the forward problem via Eq. (4) and compared the computed density profile with that obtained from our MC simulations (which were verified against previous simulation results in the literature[21]). This was done for all different combinations of the PY, VM, and HNC closures.

Figures 1(a)–1(c) show some results for the hard surface model at reduced densities $\rho_b\sigma^3$ of 0.319, 0.5745, and 0.813. As described in Sec. II D, the first closure listed was used to obtain the bulk fluid direct correlation function $C_0^{(2)}$ from the OZ equation and the second closure determined the form of the functional $B[\gamma]$ in Eq. (4). The three closure combinations shown in Fig. 1 were generally the best out of the many different ones tried. There are several trends evident from Fig. 1. The overall accuracy of the DFT predictions declines as the bulk particle density increases, and the most significant discrepancy with MC is typically seen at the point of particle-surface contact ($z = 0.5\sigma$). The VM+HNC and PY+HNC results are quite similar and both tend to overpredict the density value at contact. The PY+VM closure is the best at contact but is not always superior in predicting the structure of secondary layers.

Figure 2 shows some results for the Lennard-Jones 9-3 surface at $\rho_b\sigma^3 = 0.3$. For this model system, PY+VM underpredicts the height of the first peak while PY+HNC overpredicts it, and VM+HNC is very good throughout the entire range of z. Overall, these results are consistent with previous findings on bulk liquids in that the PY closure is most accurate for systems that are purely repulsive.[8,22]

Next, we applied the inverse analysis as described in Sec. II D to the same systems just considered in Figs. 1(a)–1(c) and 2, using the Monte Carlo data as experimental input. Figures 3(a)–3(c) show the $\varphi_{\text{ext}}^{\text{pred}}(\mathbf{r})$ results for the hard surface model. There are clearly parallels in accuracy be-

Downloaded 09 Jul 2012 to 128.119.169.61. Redistribution subject to AIP license or copyright; see http://jcp.aip.org/about/rights_and_permissions

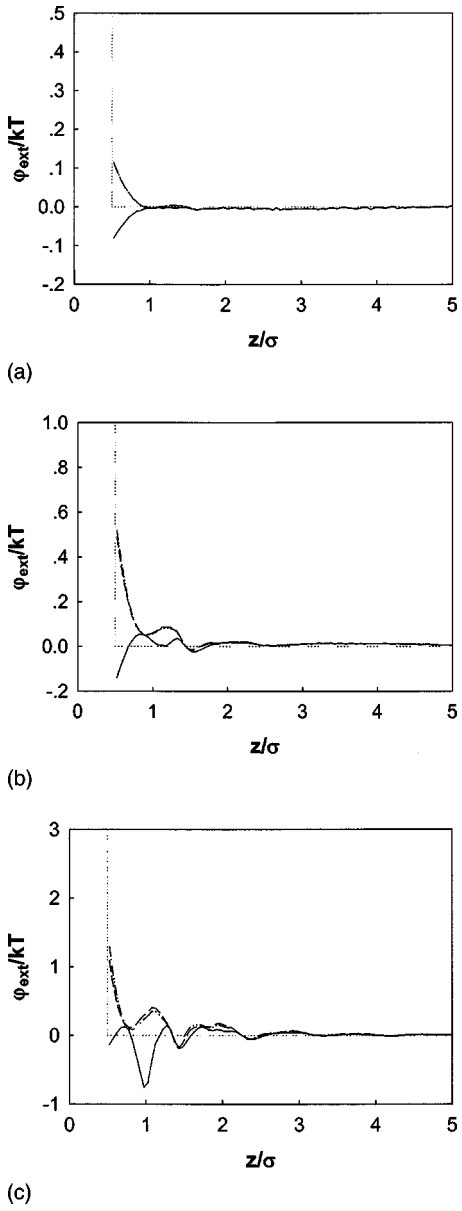

FIG. 3. Potential energy $\varphi_{ext}(z)$ of a hard sphere in contact with a hard planar surface, for bulk densities $\rho_b\sigma^3$ of (a) 0.319, (b) 0.5745, and (c) 0.813, as predicted by Eq. (5). The Monte Carlo data shown in Fig. 1 were used as input. In each case, the solid line was obtained with the PY closure for the bulk direct correlation function and VM for the bridge function (PY+VM). The dashed line and dash-dot-dot lines are for the VM+HNC and PY+HNC combinations, respectively. The light dotted line shows the exact potential energy.

tween the forward and inverse calculations. The overall accuracy of the inversion process declines as the bulk density increases, and the worst results are typically seen near contact. At the lowest bulk density the maximum error is only $0.1kT$, but at the highest bulk density the maximum error exceeds $0.5kT$ in all cases. The PY+VM closure is indeed the best near contact but predicts a deep ($\sim 0.7kT$) local minimum near $z/\sigma=1$ at the highest bulk density.

Figure 4 shows the inversion results for the Lennard-Jones 9-3 surface. The VM+HNC and PY+HNC results were nearly identical and quite good, with overpredictions of no more than $0.1kT$ along the attractive well. The PY+VM closure underpredicted the potential in this range by a slightly worse margin.

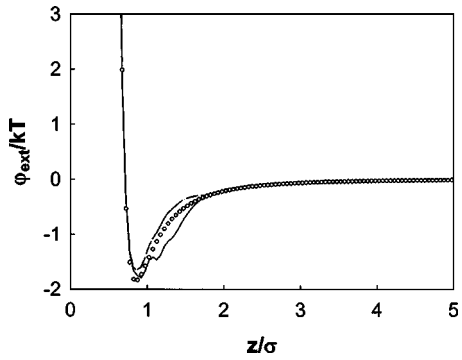

FIG. 4. Potential energy $\varphi_{ext}(z)$ of a hard sphere in contact with a Lennard-Jones 9-3 surface, as predicted by Eq. (5). The bulk density $\rho_b\sigma^3$ was 0.3; the potential model and parameter values are given in the text. The Monte Carlo data shown in Fig. 2 were used as input. As in Fig. 3, the solid, dashed, and dash-dot-dot lines denote the PY+VM, VM+HNC, and PY+HNC closure combinations, respectively. The open circles denote the exact Lennard-Jones 9-3 potential.

V. CONCLUSIONS

The recent DFT formulation of Zhou and Ruckenstein was used in an inverse mode to make predictions of particle-surface potentials from density profile information; we expect that such a process will be useful in the interpretation of optical microscopy measurements of colloidal distribution functions near surfaces. The accuracy of the predicted potential depended on the bulk particle density and the choice of DFT closure relationships. Results from hard sphere and hard surface models demonstrated that the PY+VM combination of closures would produce acceptable results ($<0.1kT$ maximum deviation from true potential) at bulk densities $\rho_b\sigma^3<0.3$ (about 1/3 of the density at the onset of the bulk freezing transition). Results from hard-sphere and Lennard-Jones surface models indicated that HNC-based closures will produce similar accuracy for attractive continuous potentials. Future work will focus on further study of the performance of closures, especially at higher bulk density, use of repulsive and attractive DLVO potentials, and application to actual experimental density profile data.

ACKNOWLEDGMENTS

One of the authors (M.A.B.) acknowledges the National Science Foundation (Grant No. CTS-0346473) and the Robert A. Welch Foundation (Grant No. A-1567) for partial support of this work. Another author (D.M.F.) thanks the Department of Energy and Sandia National Laboratories for partial support of this work through a PECASE grant. Sandia is a multiprogram laboratory operated by Sandia Corporation, a Lockheed Martin Company, for the United States Department of Energy under Contract No. DE-AC04-94AL85000.

[1] H. J. Wu and M. A. Bevan, Langmuir **21**, 1244 (2005).
[2] D. C. Prieve, Adv. Colloid Interface Sci. **82**, 93 (1999).
[3] J. C. Crocker and D. G. Grier, J. Colloid Interface Sci. **179**, 298 (1996).
[4] A. D. Dinsmore, E. R. Weeks, V. Prasad, A. C. Levitt, and D. A. Weitz, Appl. Opt. **40**, 4152 (2001).
[5] *Fundamentals of Inhomogeneous Fluids*, edited by D. Henderson (Marcel Dekker, Inc., New York, 1992).
[6] S. Q. Zhou and E. Ruckenstein, J. Chem. Phys. **112**, 8079 (2000).

Downloaded 09 Jul 2012 to 128.119.169.61. Redistribution subject to AIP license or copyright; see http://jcp.aip.org/about/rights_and_permissions

[7] M. Calleja, A. N. North, J. G. Powles, and G. Rickayzen, Mol. Phys. **73**, 973 (1991); S. Q. Zhou and E. Ruckenstein, Phys. Rev. E **61**, 2704 (2000).
[8] J.-P. Hansen and I. R. McDonald, *Theory of Simple Liquids*, 2nd ed. (Academic, London, 1996).
[9] N. Choudhury and S. K. Ghosh, J. Chem. Phys. **114**, 8530 (2001).
[10] S. Q. Zhou and E. Ruckenstein, J. Chem. Phys. **112**, 5242 (2000).
[11] S. Q. Zhou, Phys. Rev. E **63**, 051203 (2001).
[12] S. C. Kim and S. H. Suh, J. Chem. Phys. **117**, 9880 (2002).
[13] S. Q. Zhou, J. Chem. Phys. **113**, 8719 (2000).
[14] S. Q. Zhou, Eur. Phys. J. E **3**, 343 (2000); S. Q. Zhou and X. Q. Zhang, Phys. Rev. E **64**, 011112 (2001).
[15] M. A. Bevan, S. N. Petris, and D. Y. C. Chan, Langmuir **18**, 7845 (2002); M. A. Bevan and D. C. Prieve, *ibid.* **15**, 7925 (1999); **16**, 9274 (2000); M. A. Bevan and P. J. Scales, *ibid.* **18**, 1474 (2002).
[16] Y. Rosenfeld and G. Kahl, J. Phys.: Condens. Matter **9**, L89 (1997).
[17] R. Rajagopalan and K. S. Rao, Phys. Rev. E **55**, 4423 (1997); L. Reatto, D. Levesque, and J. J. Weis, Phys. Rev. A **33**, 3451 (1986).
[18] M. P. Allen and D. J. Tildesley, *Computer Simulation of Liquids* (Clarendon, Oxford, 1987).
[19] M. Schmidt, M. Dijkstra, and J. P. Hansen, J. Phys.: Condens. Matter **16**, S4185 (2004).
[20] S. Labik, A. Malijevsky, and P. Vonka, Mol. Phys. **56**, 709 (1985).
[21] R. D. Groot, N. M. Faber, and J. P. Vandereerden, Mol. Phys. **62**, 861 (1987); S. Sokolowski and J. Fischer, *ibid.* **68**, 647 (1989).
[22] M. Llanorestrepo and W. G. Chapman, J. Chem. Phys. **100**, 5139 (1994).

Downloaded 09 Jul 2012 to 128.119.169.61. Redistribution subject to AIP license or copyright; see http://jcp.aip.org/about/rights_and_permissions